Fire Technology, 58, 3039–3065, 2022

Manufactured in The United States
https://doi.org/10.1007/s10694-022-01291-6

# CFD Simulations of Fire Propagation in Horizontal Cable Trays Using a Pyrolysis Model with Stochastically Determined Geometry

*Alexandra Viitanen, VTT Technical Research Centre of Finland Ltd, P.O. Box 1000, FI-02044 Espoo, Finland*
*Simo Hostikka, Department of Civil Engineering, Aalto University, P.O. Box 12100, FI-00076 Espoo, Finland*
*Jukka Vaari*, VTT Technical Research Centre of Finland Ltd, P.O. Box 1000, FI-02044 Espoo, Finland*

**Received:** 5 May 2021/**Accepted:** 25 June 2022/**Published online:** 30 July 2022

***Abstract.*** In this paper, a pyrolysis model for a PVC cable is constructed using results from thermogravimetric analysis, microscale combustion calorimeter and cone calorimeter experiments. The pyrolysis model is used to simulate fire propagation in horizontal cable trays. The simulated arrangement corresponds to a cable tray fire experiment from OECD PRISME 2 project. As laying the cables loosely along the horizontal trays is a random process, a novel stochastic method is developed for making the simplified cable tray geometries for the computational fluid dynamics model. In addition, as the simplified cable tray geometry has significantly smaller surface area than a real tray full of cables, the surface area was parametrically adjusted. In contrast to most of the earlier published numerical approaches for simulating cable tray fires, the presented approach does not use empirical correlations for predicting fire propagation and does not require any results from full-scale experiments for calibrating the model. The simulation results are compared to experimental results in terms of heat release rate, mass loss, tray ignition times and lateral flame spread rates. The maximum heat release rate was overpredicted by 8% on average.

**Keywords:** Cable tray, Fire spread, Pyrolysis, CFD

## 1. Introduction

Electrical equipment is one of the most probable cause of fire in nuclear power plants (NPP): almost half of the fire events in NPPs reported in the OECD FIRE Database have been caused by electrical equipment [1]. Although cables have been reported to act as the fire initiator only in approximately 5% of the reported fires [1], a fire initiating at a different source may spread to cables as well. As there are

*Correspondence should be addressed to: Jukka Vaari, E-mail: jukka.vaari@vtt.fi

typically hundreds of kilometres of electrical cables in NPPs [2], they pose a significant fire load.

After the major fire at Browns Ferry Nuclear Power Plant in 1975, which damaged a large number of cables, a significant amount of both experimental and numerical work has been carried out in order to understand and predict fire propagation in cable trays. The efforts to develop numerical models for predicting cable tray fires have often been directly linked with the experimental campaigns.

In the FIPEC project, Grayson et al. [3] carried out both bench-scale and full-scale experiments and developed correlations between those. Within the same project, van Hees et al. [4] predicted the fire propagation in both bench- and full-scale using a modified version of the flame spread model developed by Yan [5], which calculated the material pyrolysis with a simple one-dimensional approach. To simulate the flame spread in the IEC 60332-3 test, the flame spread model was coupled with the computational fluid dynamics (CFD) software SOFIE [4].

McGrattan et al. [6] carried out large number of cable tray experiments in small, bench and full scale within the CHRISTIFIRE project. Within the project, an empirical FLASH-CAT model based on NUREG/CR-6850 Appendix R [7] was also developed. The FLASH-CAT model predicts heat release rate and fire propagation in horizontal cable trays in open atmosphere based on the cable type, number of trays and tray loading [6]. Modified versions of the FLASH-CAT model have been proposed for example by Zavaleta et al. [8], Plumecoq et al. [9] and Bascou et al. [10].

OECD PRISME and PRISME 2 projects have experimentally studied fire propagation in cable trays amongst other topics. The full-scale experiments have been performed for different cable types in both open atmosphere and confined, mechanically ventilated environments [2]. The topics which have been studied include horizontal and inclined trays, different ventilation rates and underventilated fires. Zavaleta and Audouin [11] and Zavaleta et al. [12] have published more thorough analysis of the cable tray fire experiments within the PRISME 2. Video analysis of the PRISME 2 cable tray fire experiments has been published both by Beji et al. [13] and Zavaleta et al. [8]. Siemon et al. [14] carried out cable tray fire experiments similar to the PRISME 2 experiments, but with alternating the arrangement of the cables and the trays.

Zavaleta et al. [8] used video analysis to obtain parameters for the FLASH-CAT model from the PRISME 2 experiments, after they had shown that the original model parameters did not result in good agreement with the experimental results. Plumecoq et al. [9] implemented FLASH-CAT into two-zone model SYLVIA for predicting fire propagation in cable trays in a confined environment but used an empirical correlation for predicting lateral fire spread after ignition to take into account the confinement effects. Bascou et al. [10] implemented a modified version of FLASH-CAT into CFD code CALIF3S/ISIS using the experimental parameters obtained by Beji et al. [13] through analysing videos of the corresponding full-scale experiments. The aim was to assess the capability of the software to predict conditions due to the known fire, while no attempt was made to predict the fire heat release rate [10].

Siemon et al. [14] simulated cable tray fires with both CFD code Fire Dynamics Simulator (FDS) and lumped parameter code Containment Code System (COCOSYS) using empirical parameters obtained through analysing videos of the corresponding full-scale experiments. Beji and Merci [15] used cone calorimeter data to predict the fire spread in cable trays with FDS. They assumed that the local burning follows the heat release rate in the cone calorimeter, or its modified version, after the surface temperature reaches the ignition temperature of the material. They demonstrated the importance of the cable tray geometry in the simulation model for predicting flame propagation correctly, although the improved geometry was made in arbitrary manner [15]. Hehnen et al. [16] simulated a cable tray fire experiment from the CHRISTIFIRE project with the CFD code FDS, using pyrolysis models which they had developed using cone calorimeter results from different test conditions [16].

Pyrolysis models have also been used to simulate cables in small- and bench-scale experiments. Matala and Hostikka [17] developed pyrolysis models for two polyvinyl chloride (PVC) cables using small-scale and bench-scale experimental data. Simulation results were validated against experimental results [17]. Pyrolysis models have also been used to predict fire behaviour of charring polymer materials, of which some are typically found in cables, in bench-scale experiments, e.g., by Stoliarov et al. [18] and Lautenberger and Fernandez-Pello [19]. Also medium-scale experiments have been simulated, e.g., Single Burning Item (SBI) test by Hjohlman et al. [20] for textile products and by Zeinali et al. [21] for fibreboard panels. Similarly, Marquis et al. [22] have used a pyrolysis model to predict fire behaviour of full-scale polymer-based composite structures.

In this paper, a full-scale simulation of a cable tray fire was conducted. Fire propagation in cable trays in open atmosphere was simulated, and the obtained results were compared with experimental results from PRISME 2. The simulations were conducted with the CFD code FDS. The thermal decomposition of the cables was predicted with a pyrolysis model, which was built based on experimental results from thermogravimetric analysis (TGA), microscale combustion calorimeter (MCC) and cone calorimeter. A simplified geometry was used to represent the cable trays in full scale. A stochastic approach was developed to create the simplified geometries for the simulation model. In addition, an area adjustment factor was used to increase the mass flux, as the simplified geometry has significantly smaller surface area than a real tray full of cables. The developed approach is meant for horizontal ladder type cable trays with loose arrangement of cables. In contrast to most of the numerical approaches for simulating cable tray fires published earlier, the presented approach does not use empirical correlations for predicting fire propagation and does not require any results from full-scale experiments for calibrating the model.

Fire propagation within a cable tray is dependent on cable arrangement both in experiments and in numerical models. Siemon et al. [14] and Huang et al. [23], amongst others, have shown that there can be a significant difference in fire behaviour between loosely and tightly arranged cable trays. To correctly represent a loose horizontal cable tray arrangement with a simple geometry, the hot gases should be able to rise through the trays and an estimate should be made for the

area of the openings. As laying the cables along the trays loosely is a random process, it is difficult to describe the result in a deterministic manner. Thus, making the stochastic model was motivated by representing the complex cable tray arrangement as correctly as possible with simple geometries.

## 2. Studied Scenario

In this study, CFSS-1 experiment from OECD PRISME 2 project was considered. The experiment was carried out by Institut de Radioprotection et de Sûreté Nucléaire (IRSN) in their DIVA facility. As the experiment and its results have been reported at length previously, e.g., by Zavaleta et al. [12], it is only shortly described here.

In the CFSS-1 experiment, a set of five horizontal cable trays, stacked vertically 30 cm apart, were burned in a large-scale calorimeter. The ladder type trays were 3 m long and 0.45 m wide. There were 49 PVC cables with length of 2.4 m in each of the trays during the test. The cables were arranged loosely in the trays. There was an insulated wall behind the trays. It had the same length as the trays and height of 3 m [12].

The cables located in the trays were MCMK 0.6/1 kV power installation cable, which has a nominal diameter of 13 mm. The cable includes three metal conductors with area of 2.5 $mm^2$. In addition to conductors, the cable consists mainly of sheath, filler and insulation materials. According to Mangs and Hostikka [24], manufacturer has reported that the sheath and insulation materials are PVC blends, but has not reported the composition of the filler material. The cable weights approximately 236 g/m, of which approximately 37% is sheath material, 15% filler material, 12% insulation material and 36% metal [24].

The lowest cable tray was ignited with a propane sand burner located below the tray. Burner was located halfway along the tray in both longitudinal and transverse directions. The burner was used at a power of 80 kW until the heat release rate from the cables exceeded 400 kW, after which the burner was turned off. The conditions in the large-scale calorimeter are considered equivalent to open atmosphere conditions due to large size of the test hall [12].

## 3. Methods

### *3.1. Numerical Method*

FDS is a large eddy simulation (LES) code, primarily meant for studying incompressible, thermally-driven flows, using low Mach number approximation. The used governing equations of the flow are conservation of mass, momentum, energy and concentration and the equation of state for an ideal gas. For more elaborate description of the theoretical approach and numerical implementation, reader is referred to the technical reference guide of the FDS software [25].

Combustion is assumed mixing controlled. The combusting gas was assumed to be propane. The combustion was assumed incomplete. The propane gas produced

by the burner was assumed to yield 0.005 g/g carbon monoxide (CO) and 0.019 g/g soot [26]. The fuel gas produced by the cables was estimated to yield 0.05 g/g CO and 0.1 g/g soot, based on the values provided for electrical cables containing PVC and polyethylene (PE) [26].

Grey gas assumption is used, i.e., spectral dependence is neglected [25]. A radiative fraction of 0.30 was used, which corresponds to pure propane [27]. While it is possible that a higher value would be more suitable, e.g., based on the work of Quintiere, Lyon and Crowley [28], to the authors' knowledge no experimental results have been published for the radiative fraction of cable fires. As the radiative fraction is likely a significant parameter for the fire propagation in the models, it was decided to not use a larger value.

An autoignition temperature (AIT) was used to prevent ignition in the simulation areas with low gas temperature. It is expected that during times when the cables are burning intensely, some fuel gas might not combust due to lack of oxygen near the flames. If AIT is not used, this fuel gas would ignite further away from the fire when there is enough oxygen available again, even if the temperature is not high enough to support autoignition. An exclusion zone for the AIT was applied around the gas burner to prevent the need for an external heat source in the simulations to simulate piloted ignition. AIT was set to 450°C, which is a typical value for propane [29].

One-dimensional heat conduction model was used. With the one-dimensional heat conduction model, conduction in direction $x$ is defined as:

$$\rho_s c_{p,s} \frac{\partial T_s}{\partial t} = \frac{\partial}{\partial x}\left(k_s \frac{\partial T_s}{\partial x}\right) + \dot{q}_s''' \tag{1}$$

where $\rho_s$ is material's component-averaged density, $c_{p,s}$ material's component-averaged specific heat, $T_s$ solid phase temperature, $t$ time, $k_s$ material component's thermal conductivity and $\dot{q}_s'''$ source term for chemical and radiative heat transfer within the solid [25].

FDS is a large eddy simulation code, which employs implicit filtering with local cell size taken as filter width. Closure for subgrid-scale stress terms is provided by using turbulence models. Variation of Deardorff's model for eddy viscosity, which has been implemented into FDS as the default turbulence model, was used [25].

Wall-adapting local eddy-viscosity (WALE) model was used as the turbulence model in the first gas phase cell in front of solids. WALE is implemented into FDS as a default near-wall turbulence model for LES simulations [25].

FDS software allows the user to define reaction mechanisms and reaction rates for the solid materials. Rate for a non-oxidative reaction $j$ of material $i$ at temperature $T_s$ is defined as:

$$r_{ij} = A_{ij} Y_{s,i}^{n_{s,ij}} exp\left(\frac{E_{ij}}{RT_s}\right) \tag{2}$$

where $A_{ij}$ is the pre-exponential factor, $Y_{s,i}$ is the mass fraction of material $i$, $n_{s,ij}$ is the reaction order, $E_{ij}$ is the activation energy and $R$ is the universal gas constant. The mass fraction of material $i$, $Y_{s,i}$, is defined as:

$$Y_{s,i} = \frac{\rho_{s,i}}{\rho_s(0)} \tag{3}$$

where $\rho_{s,i}$ is the mass of material $i$ divided by the volume of the material layer and $\rho_s(0)$ is the initial density of the material layer. The produced gaseous products are placed in the first gas cell next to the pyrolysing solid cell without mass transfer resistance [25].

### 3.2. Domain, Discretization and Boundary Conditions for Full-Scale Simulations

The geometry used for the full-scale simulations is visualized in Figure 1. The cable trays are located in the middle of the computational domain. The computational domain has height of 10 m, width of 6 m and depth of 2.4 m. The domain boundaries are positioned far enough from the fire source ensuring that the boundaries do not disturb either the flow or the combustion process. The numeri-

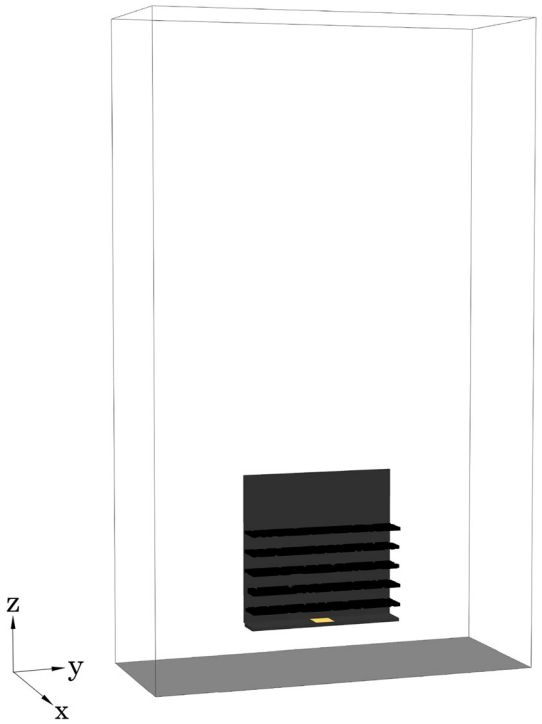


**Figure 1. Simulation domain.**

cal mesh consisted of regular hexahedral cells. The edge length of the cells was 5 cm in the vicinity of the fire and 10 cm elsewhere. The grid refinement around the cable trays is shown in Figure 2. The refined region continues to the upper end of the domain. The extent of the AIT exclusion zone in the *xz*-plane is shown as bold, dashed line in Figure 2. In the *y*-direction the zone extends over the tray length.

An upwind boundary condition is applied to the exterior boundaries of the domain, except for the exterior boundary located below the trays. With the upwind boundary condition, the gradients of tangential velocity components are zero and the pressure along outflow streamlines is constant [25]. This boundary condition is known as open boundary condition using the software specific terminology.

The floor is assumed to be 30 cm thick concrete. The insulated wall behind the trays is assumed to be 5 cm thick insulation board. The burner is assumed to be located on a steel tray, which has thickness of 5 mm. The properties used for concrete, steel and insulation board are shown in Table 1. Cable properties, presented in detail in Sect. 3.4, are applied on the top and bottom surfaces of the cable tray geometries, whereas the side surfaces are considered to be adiabatic.

The simulated physical time was 1200 s (20 min). The time step was adjusted automatically using Courant-Friedrichs-Lewy (CFL) and von Neumann stability constraints, which is the default approach for LES with FDS.

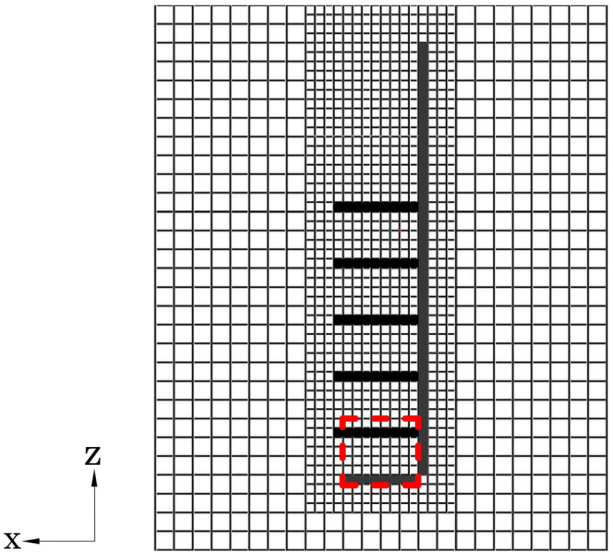


**Figure 2. Detail from the numerical grid. The refinement around the trays continues to the upper end of the domain. The extent of the AIT exclusion zone in the *xz*-plane is shown as bold, dashed line. In the *y*-direction the zone extends over the tray length.**

**Table 1**
**Properties Used for Concrete, Steel and Insulation Board**

| Material | $k$ (W/mK) | $c_p$ (kJ/kgK) | $\rho$ (kg/m$^3$) | $\epsilon$ |
|---|---|---|---|---|
| Concrete | 1.5 | 0.74 | 2430 | 0.9 |
| Steel | 45.8 | 0.46 | 7850 | 0.95 |
| Insulation board | 0.08 | 0.8 | 350 | 0.8 |

### *3.3. Simplified Cable Tray Geometry*

The used CFD software, FDS, requires that geometries conform to the rectilinear numerical grid when the standard geometrical objects are used. These geometries are known as obstructions using the software specific terminology. Conforming to the rectilinear numerical grid limits the accuracy of geometrical descriptions of objects with complex shape. Cable trays are often represented as single solid geometries, which does not allow simulating realistic fire spread in loose arrangements, as reported for example by Beji and Merci [15]. Fire spread can be simulated in more realistic manner by introducing openings to the geometries to allow the passage of hot gases. Such approaches have been presented e.g. by Beji and Merci [15], but the modelling of openings has been arbitrary.

As already mentioned in Sect. 1, previous experimental studies [14, 23] have demonstrated that the fire propagation depends on the cable arrangement. Thus, to simulate fire propagation as correctly as possible, the complex cable arrangement within the trays is represented as accurately as possible with simple geometries. As laying the cables loosely along the horizontal trays is a random process, a stochastic method was developed for making the simplified cable tray geometries.

The developed stochastic approach consists of two consecutive steps. In the first step, an estimate is made for how many openings are required in the CFD cable tray geometry. First, a volume corresponding to the known tray volume is considered, and it is represented by an auxiliary three-dimensional grid. The cell size in the auxiliary grid in both transverse and vertical direction correspond to the diameter of the studied cable. Cables corresponding to the known tray loading are divided into smaller units, which are equivalent to pieces of cable with length equal to the grid cell length in longitudinal direction. See Figure 3 for the schematic visualization of the auxiliary grid used in the stochastic model.

The units of the individual cables are sequentially placed in the grid. Their path along the tray is random, but continuity is enforced. See Figure 4 for three examples of cables that have been generated using the developed stochastic process. The curves have been drawn through the cell centres where the cable pieces have been positioned. In the auxiliary grid, a cell with a cable unit has a value of one, and an empty cell a value of zero. After all cable units have been placed, the generated three-dimensional array is made two-dimensional by summing over tray height. Using the two-dimensional array, an estimate can be made for the area of

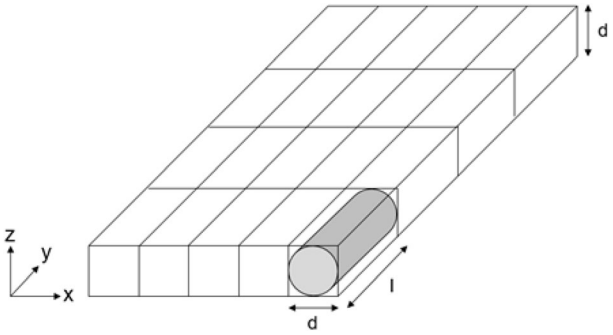


**Figure 3. Schematic visualization of the auxiliary grid used in the stochastic model.**

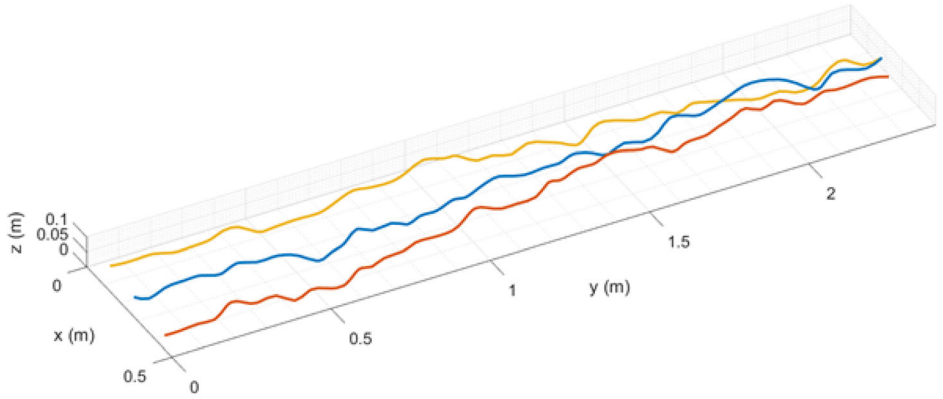


**Figure 4. Three examples of cables that have been generated using the developed stochastic process. The curves have been drawn through the cell centres where the cable pieces have been positioned.**

the openings. The estimated opening fraction, which is given as a percentage of the surface area of the whole tray, is saved. This procedure is repeated sufficient number of times to produce a statistical distribution. The average opening fraction is then used to calculate equivalent number of CFD grid cells. In the second step, the required input for making the openings for the CFD geometry is generated automatically. The locations of the openings are generated randomly, and it is checked that each opening is unique.

The presented approach was used to make the cable tray geometries. The tray dimensions and loading were taken as per Sect. 2, i.e., there were considered to be 49 cables with a nominal diameter of 13 mm in a 0.45 m wide tray. It was assumed that the maximum height of the stacked cables within a tray was 7.5 cm. Thus, if we compare volumes of the cables and volume of the tray that includes any cables (i.e. up to maximum height), the cables fill only 19.3% of the tray. The generated distribution of opening fractions is presented in Figure 5. The estima-

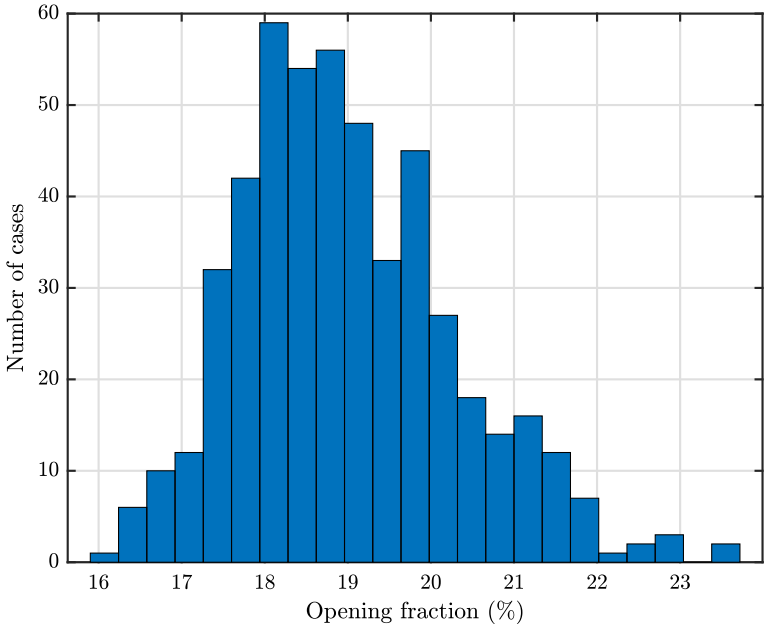


**Figure 5. Generated distribution of opening fractions when the estimation procedure was repeated 500 times. There were considered to be 49 cables with a nominal diameter of 13 mm in a 0.45 m wide tray. The maximum height of the stacked cables within a tray was 7.5 cm.**

tion procedure was repeated 500 times and the average of the obtained distribution is 19.0%. With the cell size used, this indicates that 82 solid cells should be removed. Example of a cable tray geometry generated with this approach is presented in Figure6. Visualization has been made with Smokeview software, version 6.7.14. Tray is shown from above, and black area represents solid cells.

Another issue that is caused by the low accuracy of geometrical descriptions is incorrect surface area of the cables. A single solid obstacle has significantly less exposed surface area than an equal volume filled with small cylinders, which are laid loosely enough to have most of their surface exposed. This can be addressed by parametrically adjusting the exposed surface area in the model. Similar

**Figure 6. Automatically generated tray geometry. Tray is shown from above, and black area represents solid cells.**

approach has been used by Kallada Janardhan and Hostikka [30] for predicting fire spread in wood cribs, which also have an issue with practical size of grid cells restricting the accuracy of geometrical description. Here, based on the known cable and tray dimensions, an area adjustment factor of 2.75 was used to modify the tray surface area. This value is obtained by comparing the surface areas of the cables in the experiment, assuming that the whole surface area of each individual cable is fully exposed, to the horizontal surface areas of the model geometry after the openings have been made to the geometry. While the whole circumference of the cables is not exposed in reality because of the contacts between the cables, this assumption has been made here for simplification. As the cable arrangement is loose, most of the cable surface area is exposed. It should be noted that this might not represent the way normal cable installations are done in practise, but this is how the cables were arranged in the experiment.

The area adjustment was not used with the cone calorimeter model, which causes non-continuity in the multiscale modelling process. However, if the cable surface area had been adjusted in the cone calorimeter model, it is considered that a different, smaller adjustment factor should have been used than in the full-scale model. The cables in the full-scale experiment are positioned extremely loosely in the trays and can be complete engulfed in the flame coming from the tray(s) below. In the cone calorimeter, the pieces of cables are packed extremely tightly within a metal frame, and only upper half of the cables is visible. It is suggested that if an area adjustment factor had been used in this study for the cone calorimeter model, a suitable value would have been approximately 1.5.

### *3.4. Pyrolysis Model*

A pyrolysis model is needed to model thermal decomposition of a material. The approach which has been used here for making the pyrolysis model can be outlined as follows. First, the material structure and components are chosen. If the material has a complex structure, it can be simplified by reducing the number of layers or material components. After the material components have been chosen, reaction paths are formed for each component. As the actual chemical reactions are not known, reactions are chosen by the modeller. Similar approach was followed by Matala and Hostikka [17], who note that the chosen reaction scheme can be assessed based on the model's fitting capability. Here, the reaction paths were formed using results from TGA and MCC. After the reaction paths have been formed, kinetic parameters are estimated for each reaction based on the TGA results. As the model aims to capture correctly only the mass consumption during the reactions, kinetic parameters are allowed to take values which could be considered unphysically low or high. After suitable kinetic parameters have been found, the remaining unknown parameters are estimated based on the cone calorimeter results. Here, estimations have been made for heats of reaction, heats of combustion, specific heats and thermal conductivities.

The cable is represented by a regular hexahedron geometry. The simplified cable is assumed to consist of four different materials in seven different layers. The structure of the simplified cable is symmetric with respect to the centreline of the

material. It is assumed that the layers from external side to the centre are sheath, filler, insulation and copper. A schematic visualization of the simplified cable structure is shown in figure 7. Thicknesses of the material layers are in proportion to each other in the figure. In the cone calorimeter simulation, thicknesses of the layers are assumed to be 1.8 mm for insulation material in total, 5.8 mm for the sheath material in total, 2.4 mm for the filler material in total and 0.8 mm for the copper. With these values, correct total mass and component mass fractions are obtained.

Reaction paths were formed for polymeric cable materials using the principles presented by Matala and Hostikka [17], i.e., the reaction paths were kept as simple as possible and were assessed based on their capability to reproduce the experimental results. It was assumed that each of the materials initially consist of single component, and that all reactions happen in a single step. The components in the virgin materials are referred to as *Sheath component 1*, *Insulation component 1* and *Filler component 1*. The other components are the residue components from the previously decomposed materials: for example, when *Sheath component 1* decomposes, 25% of the mass is released as gaseous fuel, 29% of the mass is released as inert gas and the remaining solid residue (46%) becomes *Sheath component 2*. The amount of mass consumed in each reaction step was evaluated from the TGA results by Mangs and Hostikka [24]. Based on the MCC results by Mangs and Hostikka [24], estimations were made for how much of the released gas is fuel and how much is inert gas. A heat of combustion of 45 MJ/kg was used for the fuel. The yields of reactions and the names of residue components are shown in Table 2.

To find the kinetic parameters, the TGA was simulated with FDS, version 6.7.3, using the method proposed in the FDS User Guide [31]. Optimisation tool PyroPython was used for parameter optimisation. PyroPython is designed to efficiently optimise black-box functions and has been specifically made for pyrolysis parameter estimation. PyroPython is available as an open source tool [32]. Goodness of the fit was evaluated based on the difference between the experimental and simulated mass loss as a function of temperature. Only the kinetic parameters $A$, $E$ and $n_s$ were optimised. A Bayesian optimisation algorithm was used. The obtained kinetic parameters for the polymeric cable components are presented in Table 3.

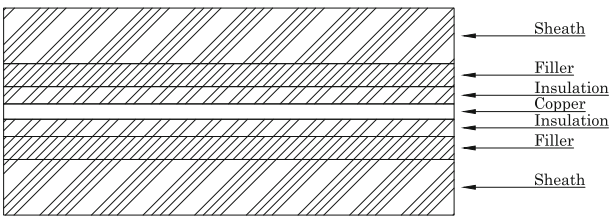


**Figure 7. Schematic visualization of the simplified cable structure. Thicknesses of the material layers are in proportion to each other.**

**Table 2**
**Yields of Reactions and Residue Components**

| Component | Fuel (%) | Inert gas (%) | Residue (%) (residue component) |
|---|---|---|---|
| Sheath component 1 | 25 | 29 | 46 (Sheath component 2) |
| Sheath component 2 | 23 | 3 | 74 (Sheath component 3) |
| Sheath component 3 | – | 29 | 71 (Char) |
| Insulation component 1 | 19 | 26 | 55 (Insulation component 2) |
| Insulation component 2 | 16 | 2 | 82 (Insulation component 3) |
| Insulation component 3 | – | 26 | 74 (Char) |
| Filler component 1 | 12 | 12 | 76 (Filler component 2) |
| Filler component 2 | 4 | 1 | 95 (Filler component 3) |
| Filler component 3 | – | 3 | 97 (Filler component 4) |
| Filler component 4 | 3 | 34 | 63 (Char) |

**Table 3**
**Kinetic Parameters of the Polymeric Cable Components**

| Component | $A$ (1/s) | $E$ (J/mol) | $n_s$ (−) |
|---|---|---|---|
| Sheath component 1 | $7.0 \times 10^{32}$ | $3.8 \times 10^{5}$ | 2.4 |
| Sheath component 2 | $2.0 \times 10^{31}$ | $4.6 \times 10^{5}$ | 2.2 |
| Sheath component 3 | $1.2 \times 10^{31}$ | $6.0 \times 10^{5}$ | 2.0 |
| Insulation component 1 | $3.9 \times 10^{21}$ | $2.5 \times 10^{5}$ | 1.1 |
| Insulation component 2 | $1.8 \times 10^{37}$ | $5.6 \times 10^{5}$ | 4.8 |
| Insulation component 3 | $4.0 \times 10^{24}$ | $5.0 \times 10^{5}$ | 2.9 |
| Filler component 1 | $2.2 \times 10^{27}$ | $3.1 \times 10^{5}$ | 3.0 |
| Filler component 2 | $4.2 \times 10^{39}$ | $5.7 \times 10^{5}$ | 3.6 |
| Filler component 3 | $7.1 \times 10^{22}$ | $4.5 \times 10^{5}$ | 3.0 |
| Filler component 4 | $1.2 \times 10^{42}$ | $2.6 \times 10^{5}$ | 3.3 |

The experimental and simulated normalized mass of insulation material as a function of temperature during the TGA are shown in Figure 8. Similar results for sheath are shown in Figure 9 and for filler in Figure 10. For the insulation, the estimation algorithm has been able to accurately reproduce the shapes of the reaction steps. For the sheath material, the second reaction has a different rate in experiment and simulation, but the third reaction is not affected by this. For the filler material, the results begin to diverge after the first reaction. The residue mass at the end is higher in the simulation than in the experiment, although the reaction yields have been taken from the experimental results. This is caused by the optimised reaction rate being slower than the experimental one, due to which the reaction has not proceeded to end before end of the simulation.

Heats of combustion and heats of reaction for polymeric cable components and thermal parameters for char were estimated using a cone calorimeter simulation and data from cone calorimeter experiments. In the cone calorimeter experiments an external flux of 50 kW/m$^2$ was used [24].

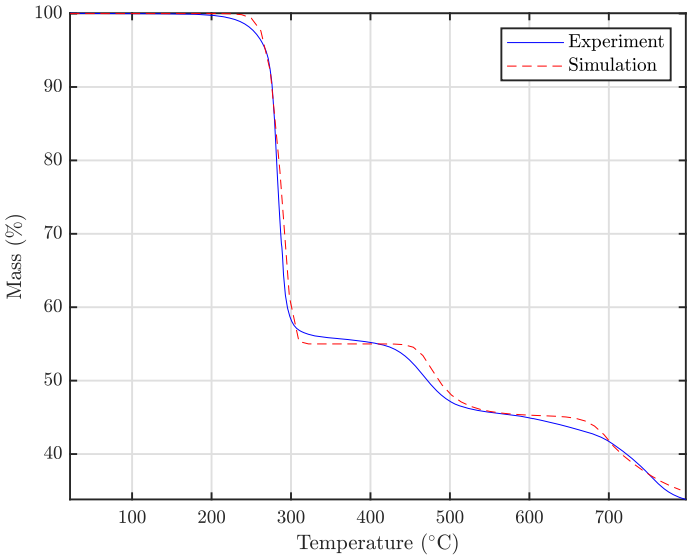


**Figure 8. Experimental and simulated normalized mass of insulation material as a function of temperature during TGA.**

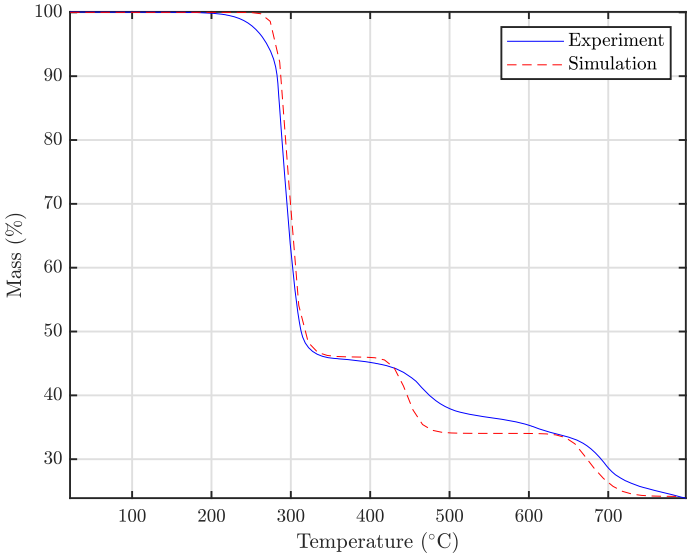


**Figure 9. Experimental and simulated normalized mass of sheath material as a function of temperature during TGA.**

The cone calorimeter experiment was simulated by using an ideal external flux on top of the specimen in similar manner as described in the FDS User Guide [31]. However, also the gas phase was modelled to include the heat from the flame

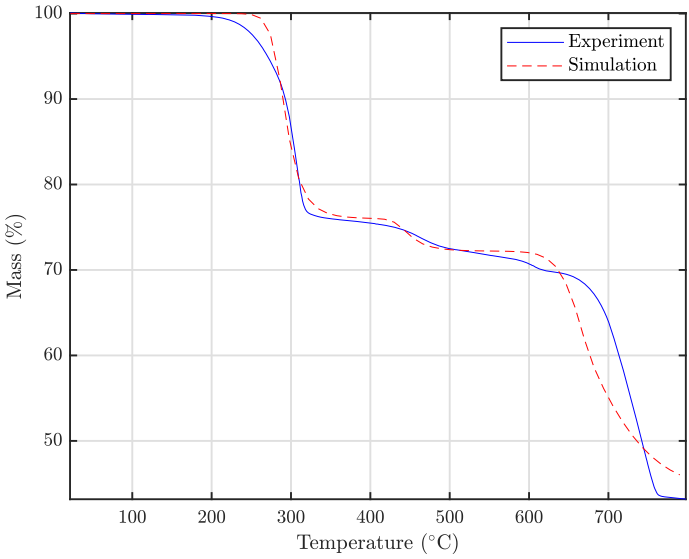


**Figure 10. Experimental and simulated normalized mass of filler material as a function of temperature during TGA.**

after the specimen ignition. Regular hexahedral cells with edge length of 5 cm were used. The modelled domain had width and length of 15 cm, and height of 40 cm. The specimen, modelled as a plane with width and length of 10 cm, was located at the bottom of the domain, in the middle. The estimation process was conducted in similar manner as the kinetic parameter estimation process, which was previously described.

Simulated and experimental heat release rates during the cone calorimeter test are shown in Figure 11. The similarity between simulated and experimental heat release rates is considered satisfactory. Simulated and experimental cable mass during the cone calorimeter test are shown in Figure 12. Mass during the experiment has been normalized with the initial mass. The simulated mass loss does not accurately follow the experimental values during the test, but as the mass loss at the end of the test is similar for both simulation and experiment, the model is considered sufficient.

The heats of combustion and the heats of reaction for the polymeric cable components are shown in Table 4. The reactions are endothermic. Density used for all polymeric cable components is 1209 kg/m$^3$, which was calculated using the known cable dimensions, component fractions and copper density. The thermal conductivities and specific heats used for the polymeric cable components are shown in Tables 5 and 6 , respectively. Properties used for char and chopper are shown in Table 7.

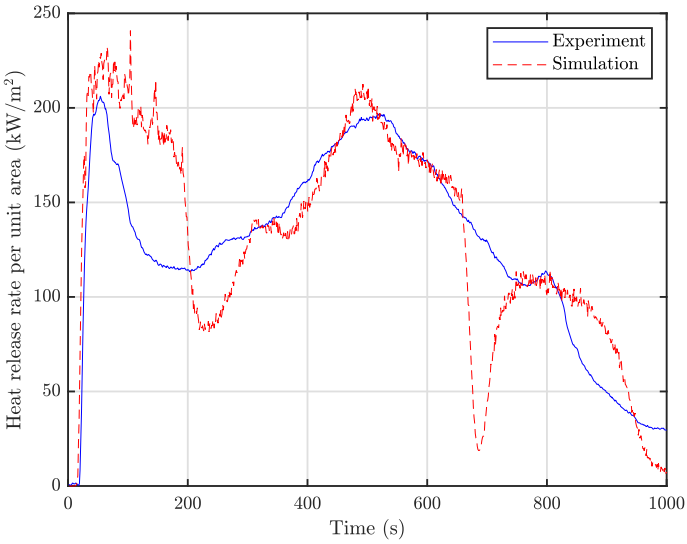


**Figure 11. Experimental and simulated heat release rate during the cone calorimeter test.**

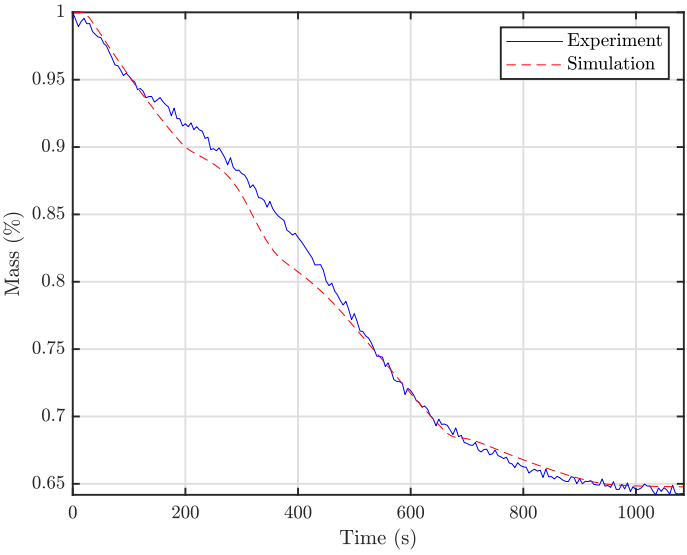


**Figure 12. Experimental and simulated mass of cables during the cone calorimeter test. Mass has been normalized by the initial mass.**

**Table 4**
**Heats of Combustion and Reaction for the Polymeric Cable Components**

| Component | $\Delta H_c$ (MJ/kg) | $\Delta H_r$ (kJ/kg) |
|---|---|---|
| Sheath component 1 | 40 | 1200 |
| Sheath component 2 | 44 | 1700 |
| Sheath component 3 | – | 380 |
| Insulation component 1 | 11 | 360 |
| Insulation component 2 | 33 | 680 |
| Insulation component 3 | – | 530 |
| Filler component 1 | 40 | 1400 |
| Filler component 2 | 17 | 360 |
| Filler component 3 | – | 620 |
| Filler component 4 | 41 | 690 |

**Table 5**
**Thermal Conductivities of Polymeric Cable Components**

| Material | $k$ at 20°C (W/mK) | $k$ at 300°C (W/mK) | $k$ at 600°C (W/mK) |
|---|---|---|---|
| Sheath | 0.13 | 0.31 | 0.71 |
| Insulation | 0.24 | 0.68 | 0.88 |
| Filler | 0.17 | 0.37 | 0.42 |

**Table 6**
**Specific Heats of Polymeric Cable Components**

| Material | $c_p$ at 20°C (kJ/kgK) | $c_p$ at 300°C (kJ/kgK) | $c_p$ at 600°C (kJ/kgK) |
|---|---|---|---|
| Sheath | 0.86 | 2.80 | 4.66 |
| Insulation | 1.85 | 2.99 | 3.48 |
| Filler | 0.16 | 1.38 | 1.99 |

**Table 7**
**Properties Used for Char and Copper**

| Material | $k$ (W/mK) | $c_p$ (kJ/kgK) | $\rho$ (kg/$m^3$) | $\epsilon$ |
|---|---|---|---|---|
| Char | 0.25 | 4.54 | 128 | 0.43 |
| Copper | 386 | 0.38 | 8954 | 1.0 |

# 4. Full-Scale Simulation Results

## 4.1. Heat Release Rate and Mass Loss

Five simulations were conducted using the same opening fraction but different randomly generated tray geometries. The cable tray geometries were generated using the procedure described in Sect. 3.3. Simulations were made with FDS, version 6.7.3. The experimental and simulated heat release rates are shown in Figure 13. It can be observed that the fire growth phase before 190 s is quite well captured in all simulations. The maximum heat release rate is overpredicted by 5.4 to 12.8%, with the average overprediction of 8.3%. The predicted fires extinguish after approximately 720 s, whereas the experimental fire was maintained until more than 1200 s had passed.

Some of the differences between the full-scale experiment and the corresponding simulations could be due to the pyrolysis model. It has been remarked by Ghorbani et al. [33] that pyrolysis models often are unable to predict behaviour correctly outside the calibration domain. As the pyrolysis model used in this work is based on experiments conducted only at a single radiation level, it might be incapable to predict thermal decomposition correctly at other, especially lower, radiation intensities. This might explain the differences seen in Figure 13 between the simulations and experiment during the decay phase.

Experimental and simulated cable mass during the full-scale test are shown in Figure 14. The mass has been normalized by the initial mass. In the experiment, 40% of the cable mass was consumed, while the simulated consumptions were approximately 47%.

Larger amount of mass is consumed in the full-scale simulations than in the corresponding experiment, although the mass consumption was correctly predicted

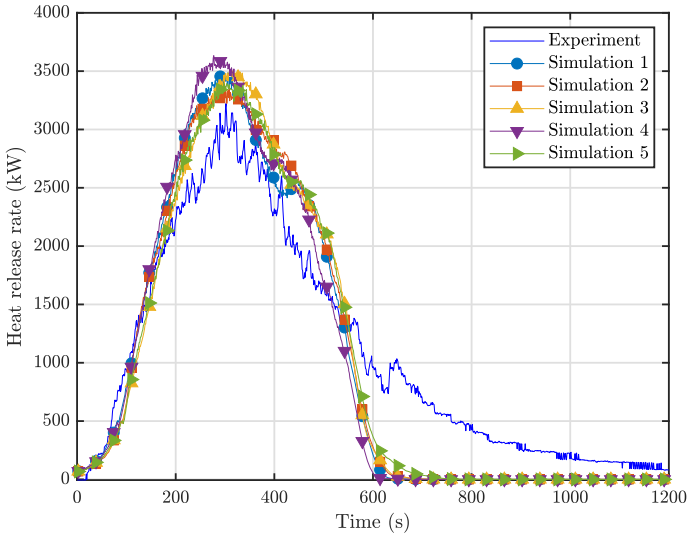


**Figure 13. Experimental and simulated heat release rate.**

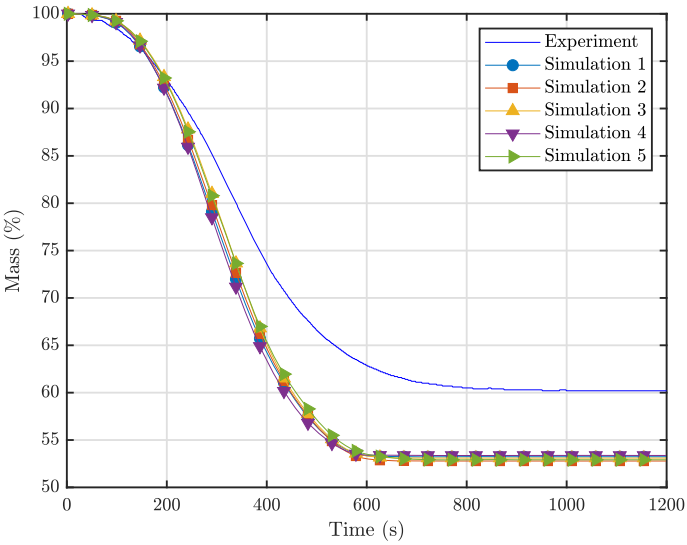


**Figure 14. Experimental and simulated cable mass during the full-scale test. The mass has been normalized by the initial mass.**

for the cone calorimeter experiment. An important aspect where the simulations of cone calorimeter and full-scale experiments differ, is that for the full-scale simulations the surface area has been parametrically adjusted, but for the cone calorimeter experiment it has been not. The assumption which was used in the adjustment was that the whole surface area of each individual cable is exposed. Given the arrangement of the cables within the trays, such as cables being partially in physical connection with each other, it could be that using some fraction of the cable surface area would be more realistic. Reducing the area used would lead to smaller mass fluxes, which would decrease the fire spread rate and the heat release rate. It should also be considered that in this study, the area adjustment factor was not used in the cone calorimeter model during the making of the pyrolysis model. This discrepancy adds uncertainty to the simulation results, and consistent use of the adjustment factor would have likely led to smaller heat release rates.

Another important aspect where simulations differ, is that in the full-scale simulations the cables are simplified as a single geometry which is continuous through the tray height. In the cone calorimeter experiment the cables are tightly arranged in a single layer, whereas in the full-scale experiment the cables are loosely arranged and there are multiple layers of cables. It could be that approximating the cables as a continuum is more suitable for modelling fire propagation in tight arrangements and leads to too high propagation rate in loose arrangements.

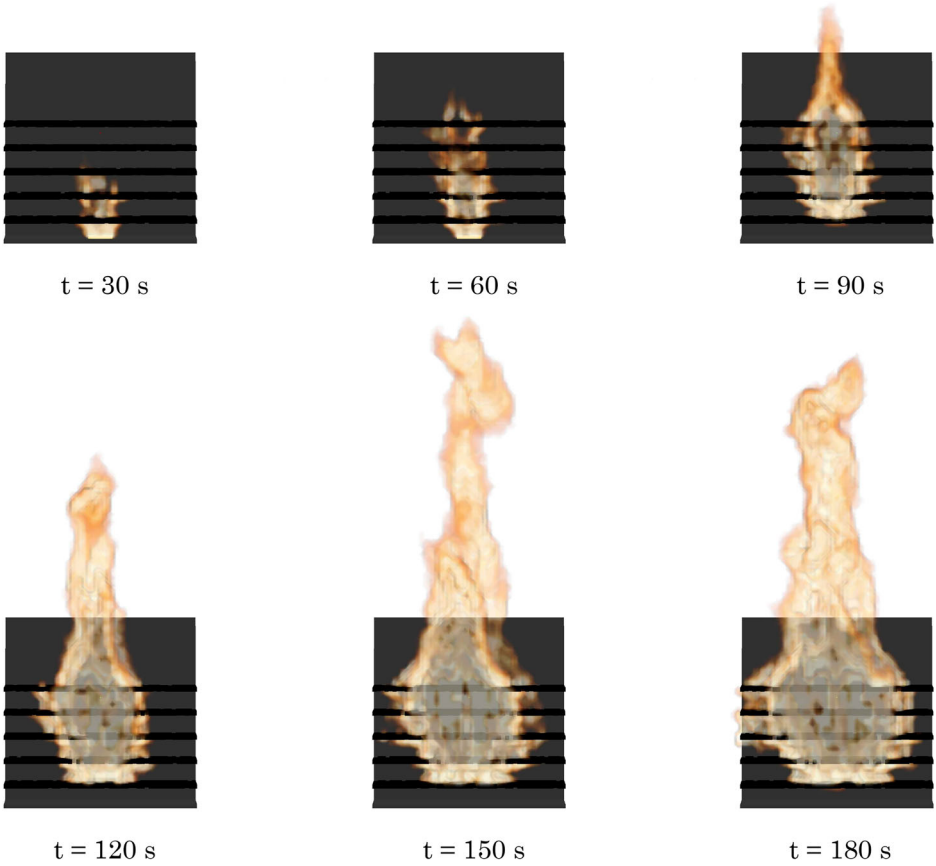


**Figure 15. Flame spread every 30 s until 180 s in *Simulation 1*. The domain boundaries and the floor beneath the trays have been omitted from the figures. After 60 s, the gas burner below the trays has been removed from the simulation.**

### *4.2. Simulated Propagation of Flame and Pyrolysis Front*

Simulated flame propagation every 30 s until 180 s in *Simulation 1* is shown in Figure 15. The domain boundaries and the floor beneath the trays have been omitted from the figures. After 60 s, the gas burner below the trays has been removed from the simulation. Trays ignite sequentially, with the lowest tray igniting first, which is physically correct behaviour. V pattern, observed in multiple cable tray experiments, can be seen in the figures although it seems to be asymmetric. Lateral flame propagation has higher rate in the upper trays than in the lower trays, which is in line with experimental observations.

To quantitatively compare the simulated and experimental values, the tray ignition times and the lateral flame spread rates within the trays were assessed. The simulated propagation of pyrolysing region was correlated to flame propagation,

which is not explicitly simulated, to allow comparison between the simulated and experimental values. The experimental values by Zavaleta et al. [8] that have been obtained through video analysis were used as reference. Using the criterion of fuel mass flux exceeding 1.7E-3 kg/s/m$^2$ to indicate sustained flame, ignition times and flame spread rates were obtained for each tray from all of the simulations. The fuel mass flux criterion is based on the cone calorimeter results. Simulated and experimental ignition times and flame spread rates are shown in Table 8. An average value from all of the simulations is shown. Tray number 1 is the lowest.

Values on both the upper and lower surfaces of the geometries representing the cable trays in the simulations have been analysed: averaged value is shown for each tray for both ignition time and flame spread rate. Flame spread rate has been calculated from the tray centre to both ends of the tray, and average of the values is used. Lower surface of tray 1 does not sustain flame in any of the simulations after the burner is removed, but it reignites in all of the simulations at approximately 180 s. To have meaningful comparison with the experimental values, the time of first ignition is used for calculating the average ignition time for the tray and the reignition time is used for calculating the flame spread rate.

In comparison to experimental values, the simulated ignition times have an average difference of 22.4% and the simulated flame spread have an average difference of 37.4%. The simulated lateral flame propagation rates are connected to the simulated heat release rates. When the heat release rate is larger in the simulation than in the experiment, the heat feedback back to the surface from the flames is also higher and in turn accelerates the flame spread. As the tray ignitions occur before the experimental and simulated heat release rates begin to diverge, they are not affected.

## 5. Sensitivity Studies

### *5.1. Opening Fraction*

To assess the sensitivity of the proposed method to the chosen opening fraction, *Simulation 1* was modified. A normal distribution was fitted to the data shown in Figure 5, and a distribution with standard deviation of 1.3% was obtained. Thus, the values one standard deviation below and above the distribution average are

**Table 8**
**Simulated and Experimental Ignition Times $t_{ig}$ (s) and Flame Spread Rates $f_s$ (mm/s) for the Cable Trays**

| | Tray 1 | Tray 2 | Tray 3 | Tray 4 | Tray 5 |
|---|---|---|---|---|---|
| $t_{ig}$, sim. (s) | 19 ± 2 | 38 ± 3 | 64 ± 6 | 83 ± 6 | 90 ± 4 |
| $t_{ig}$, exp. (s) [8] | 40 | 58 | 66 | 72 | 86 |
| $f_s$, sim. (mm/s) | 3.9 ± 0.3 | 5.1 ± 0.4 | 6.8 ± 0.5 | 8.1 ± 0.7 | 8.2 ± 0.8 |
| $f_s$, exp. (mm/s) [8] | 3.0 | 2.9 | 4.9 | 6.3 | 7.1 |

Experimental values have been obtained by Zavaleta et al. [8] through video analysis. Tray number 1 is the lowest

17.7% and 20.3%, respectively. With the used grid size, this is equivalent to having six openings more or less per tray. Two modified versions of *Simulation 1* were made with corresponding changes. In addition, a simulation without openings in the tray geometries was made for comparison.

The heat release rates for the modified versions of *Simulation 1*, the original simulation and the experiment are shown in Figure 16. In the modified cases with six openings more or less, the difference in the maximum heat release rate is approximately 1% in comparison to the original simulation. Note that to isolate the effect of the opening fraction, the material thickness and area adjustment factor were not modified correspondingly. This results in approximately 1.7% error in both cable mass and area adjustment factor per tray.

The maximum heat release rate in the simulation without openings is approximately 18% less than in the original simulation. Furthermore, the peak HRR is delayed by approximately 360 s. It takes more than 5 min for the upper surface of the second tray from below to ignite, i.e., the fire does not propagate in a realistic manner.

It was also assessed how changing the assumptions about the tray volume affects the opening fraction. The procedure described in Sect. 3.3 was repeated 100 times with the auxiliary grid modified in the vertical direction. When the cables were assumed to be in one more layer in the vertical direction than originally, the mean opening fraction was 20.4%. When the cables were assumed to be in one

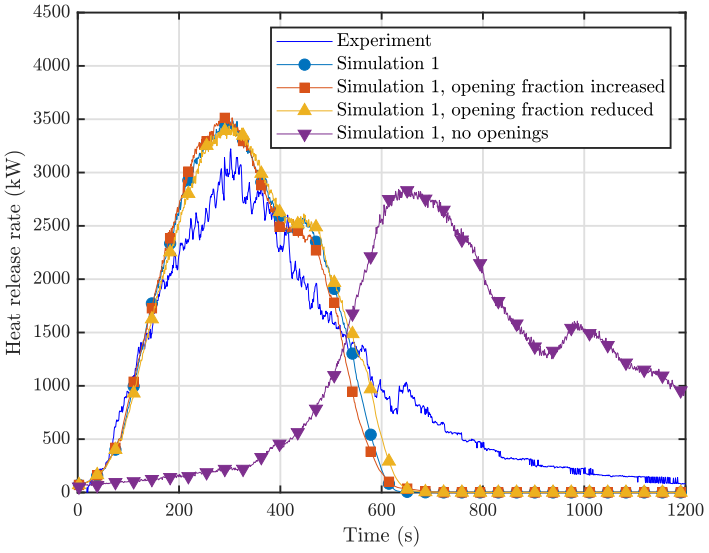


**Figure 16. Heat release rates for the modified versions of *Simulation 1*, the original simulation and the experiment. In the two first modified simulations, opening fractions one standard deviation below and above distribution average have been used. Distribution average was used in the original *Simulation 1*. In the third modified simulation, the openings in the tray geometries have been removed.**

layer less in the vertical direction, the obtained opening fraction was 18.9%. As the differences in the opening fraction are similar as in the tested cases described above, no new simulations were made.

### *5.2. Tray Surface Area Adjustment*

To assess the sensitivity of the proposed method to the chosen area adjustment factor, *Simulation 1* was modified by reducing the factor by 10%. The heat release rates for the modified *Simulation 1*, the original simulation and the experiment are shown in Figure 17. The difference in the maximum heat release rate is approximately 9.4% in comparison to the original simulation.

## 6. Conclusions

In this paper, fire propagation in full-scale cable trays was simulated using a pyrolysis model. The pyrolysis model used in the simulations was constructed using results from thermogravimetric analysis, microscale combustion calorimeter and cone calorimeter experiments. To simulate fire propagation within the cable trays correctly, the complex cable arrangements were modelled as accurately as possible. A novel stochastic approach was developed for creating the simplified tray geometries. In addition, as the simplified cable tray geometry has significantly smaller surface area than a real tray full of cables, the surface area was parametrically adjusted. The presented approach did not use empirical correlations for pre-

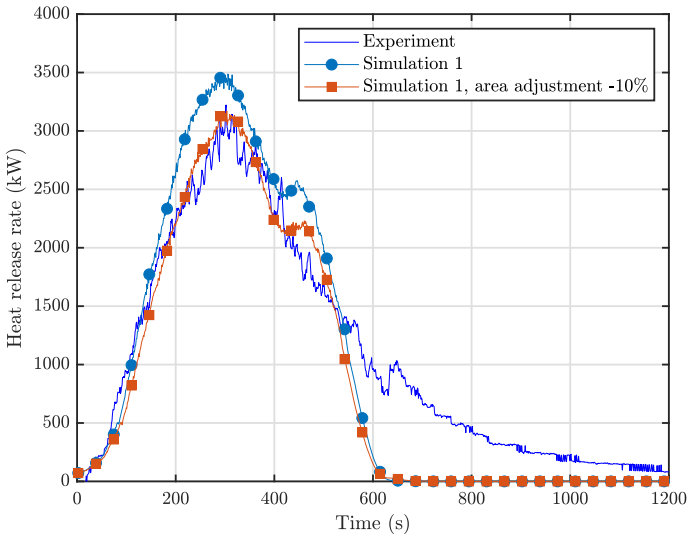


**Figure 17. Heat release rates for the modified versions of *Simulation 1*, the original simulation and the experiment. In the modified simulation the area adjustment factor has been reduced by 10%.**

dicting fire propagation nor does it require any results from full-scale experiments for calibrating the model.

The maximum heat release rate was overpredicted by 5.4 to 12.8%, with the average overprediction of 8.3%. The simulated mass consumptions were approximately 47%, whereas in the experiment 40% of the cable mass was consumed. In comparison to experiments, the simulated ignition times have an average difference of 22.4% and the simulated flame spread rates have an average difference of 37.4%.

Fire propagated faster in the full-scale simulations than in the corresponding experiments. In comparison, the heat release rate and mass consumption were predicted more accurately in the cone calorimeter simulation. It is considered possible that approximating the cables as a continuum is more suitable for modelling fire propagation in tight arrangements and leads to too high propagation rate in loose arrangements. Another aspect which could partially explain this difference is that in full-scale simulation the exposed cable area was parametrically increased, whereas in the bench-scale simulation it was not. Based on the sensitivity study, changing the area adjustment parameter has a significant effect on the results. Furthermore, the pyrolysis model used in this work is based on a very limited set of experimental data, which could limit its predictive capability.

In comparison to work of Hehnen et al. [16], who have also simulated fire propagation in cable trays using a pyrolysis model, major differences between the approaches are the use of an area adjustment factor and modified tray geometries in this work. However, the cable tray arrangements simulated in this work and by Hehnen et al. are also different.

In further work, the presented approach should be generalized for different cable types and tray arrangements. The pyrolysis model used in the simulations should be formulated using experimental data from different testing conditions to improve the accuracy of the model. The consistent use of the area adjustment factor should be implemented to reduce the uncertainty related to the proposed modelling approach.

## Acknowledgements

Partial funding for this work was received from State Nuclear Waste Management Fund through the SAFIR2022 programme. Thanks to OECD PRISME 2 project and its members for the results from the full-scale cable tray experiments.

## Funding

Open Access funding provided by Technical Research Centre of Finland (VTT).

## References

1. OECD (2015) Collection and analysis of fire events (2010–2013)—extensions in the database and applications. Fire project report. Committee on the Safety of Nuclear Installations (CSNI), NEA/CSNI/R(2015)14. https://www.oecd-nea.org/nsd/docs/2015/csni-r2015-14.pdf
2. OECD (2018) Investigating heat and smoke propagation mechanisms in multi-compartment fire scenarios. Final report of the PRISME Project, Committee on the Safety of Nuclear Installations (CSNI),NEA/CSNI/R(2017)14. https://www.oecd-nea.org/nsd/docs/2017/csni-r2017-14.pdf
3. Grayson SJ, Van Hees P, Green AM, Breulet H, Vercellotti U (2001) Assessing the fire performance of electric cables (FIPEC). Fire Mater 25(2):49–60. https://doi.org/10.1002/fam.756
4. Van Hees P, Axelsson J, Green AM, Grayson SJ (2001) Mathematical modelling of fire development in cable installations. Fire Mater 25(4):169–178. https://doi.org/10.1002/fam.767
5. Yan Z (1999) Numerical modeling of turbulent combustion and flame spread. PhD thesis, Lund University, Lund, Sweden
6. McGrattan K, Lock A, Marsh N, Nyden M, Bareham S, Morgan AB, Galaska M, Schenck K (2012) Cable heat release, ignition, and spread in tray installations during fire (CHRISTIFIRE) Phase 1: horizontal trays, NUREG/CR-7010, vol 1. Tech. rep, Office of Nuclear Regulatory Research
7. EPRI, NRC (2005) EPRI/NRC-RES fire PRA methodology for nuclear power facilities: volume 2: detailed methodology, EPRI TR-1011989 and NUREG/CR-6850. Electric Power Research Institute (EPRI), Palo Alto, CA, and US Nuclear Regulatory Commission, Office of Nuclear Regulatory Research (RES), Rockville, MD
8. Zavaleta P, Hanouzet R, Beji T (2019) Improved assessment of fire spread over horizontal cable trays supported by video fire analysis. Fire Technol 55(1):233–255. https://doi.org/10.1007/s10694-018-0788-x
9. Plumecocq W, Audouin L, Zavaleta P (2019) Horizontal cable tray fire in a well-confined and mechanically ventilated enclosure using a two-zone model. Fire Mater 43(5):530–542. https://doi.org/10.1002/fam.2698

10. Bascou S, Zavaleta P, Babik F (2019) Cable tray FIRE tests simulations in open atmosphere and in confined and mechanically ventilated compartments with the CALIF3S/ISIS CFD software. Fire Mater 43(5):448–465. https://doi.org/10.1002/fam.2680
11. Zavaleta P, Audouin L (2018) Cable tray fire tests in a confined and mechanically ventilated facility. Fire Mater 42(1):28–43. https://doi.org/10.1002/fam.2454
12. Zavaleta P, Suard S, Audouin L (2019) Cable tray fire tests with halogenated electric cables in a confined and mechanically ventilated facility. Fire Mater 43(5):543–560. https://doi.org/10.1002/fam.2717
13. Beji T, Verstockt S, Zavaleta P, Merci B (2016) Flame spread monitoring and estimation of the heat release rate from a cable tray fire using video fire analysis (vfa). Fire Technol 52(3):611–621. https://doi.org/10.1007/s10694-015-0538-2
14. Siemon M, Riese O, Forell B, Krönung D, Klein-Heßling W (2019) Experimental and numerical analysis of the influence of cable tray arrangements on the resulting mass loss rate and fire spreading. Fire Mater 43(5):497–513. https://doi.org/10.1002/fam.2689
15. Beji T, Merci B (2019) Numerical simulations of a full-scale cable tray fire using small-scale test data. Fire Mater 43(5):486–496. https://doi.org/10.1002/fam.2687
16. Hehnen T, Arnold L, La Mendola S (2020) Numerical fire spread simulation based on material pyrolysis-an application to the christifire phase 1 horizontal cable tray tests. Fire . https://doi.org/10.3390/fire3030033
17. Matala A, Hostikka S (2011) Pyrolysis modelling of pvc cable materials. In: Fire safety science, international association for fire safety science, pp 917–930. https://doi.org/10.3801/IAFSS.FSS.10-917
18. Stoliarov SI, Crowley S, Lyon RE, Linteris GT (2009) Prediction of the burning rates of non-charring polymers. Combust Flame 156(5):1068–1083. https://doi.org/10.1016/j.combustflame.2008.11.010
19. Lautenberger C, Fernandez-Pello C (2009) Generalized pyrolysis model for combustible solids. Fire Saf J 44(6):819–839. https://doi.org/10.1016/j.firesaf.2009.03.011
20. Hjohlman M, Andersson P, van Hees P (2011) Flame spread modelling of complex textile materials. Fire Technol 47(1):85–106. https://doi.org/10.1007/s10694-009-0128-2
21. Zeinali D, Gupta A, Maragkos G, Agarwal G, Beji T, Chaos M, Wang Y, Degroote J, Merci B (2019) Study of the importance of non-uniform mass density in numerical simulations of fire spread over mdf panels in a corner configuration. Combust Flame 200:303–315. https://doi.org/10.1016/j.combustflame.2018.11.020
22. Marquis DM, Pavageau M, Guillaume E (2012) Multi-scale simulations of fire growth on a sandwich composite structure. J Fire Sci 31(1):3–34. https://doi.org/10.1177/0734904112453010
23. Huang X, Zhu H, Peng L, Zheng Z, Zeng W, Bi K, Cheng C, Chow W (2019) Burning behavior of cable tray located on a wall with different cable arrangements. Fire Mater 43(1):64–73. https://doi.org/10.1002/fam.2669
24. Mangs J, Hostikka S (2013) Experimental characterization of the MCMK cable for fire safety assessment, VTT research report VTT-R-06873-12
25. McGrattan K, Hostikka S, Floyd J, McDermott R, Vanella M (2019) Fire dynamics simulator technical reference guide volume 1: mathematical model—NIST special publication 1018-1, 6th edn. Tech. rep
26. Hurley MJ, Gottuk D, Hall JR, Harada K, Kuligowski E, Puchovsky M, Torero J, Watts JM, Wieczorek C (2016) SFPE handbook of fire protection engineering, 5th edn. Springer, New York
27. Beyler C (2016) Fire hazard calculations for large, open hydrocarbon fires. In: Hurley MJ, Gottuk D, Hall JR, Harada K, Kuligowski E, Puchovsky M, Torero J, Watts JM,

Wieczorek C (eds) SFPE handbook of fire protection engineering, 5th edn, Springer, New York
28. Quintiere JG, Lyon RE, Crowley SB (2016) An exercise in obtaining flame radiation fraction from the cone calorimeter. Fire Mater 40(6):861–872. https://doi.org/10.1002/fam.2350
29. Beyler C (2016) Flammability limits of premixed and diffusion flames. In: Hurley MJ, Gottuk D, Hall JR, Harada K, Kuligowski E, Puchovsky M, Torero J, Watts JM, Wieczorek C (eds) SFPE handbook of fire protection engineering, 5th edn, Springer, New York, chap 17, pp 529–553
30. Kallada Janardhan R, Hostikka S (2019) Predictive computational fluid dynamics simulation of fire spread on wood cribs. Fire Technol 55(6):2245–2268. https://doi.org/10.1007/s10694-019-00855-3
31. McGrattan K, Hostikka S, Floyd J, McDermott R, Vanella M (2019) Fire dynamics simulator user's guide—NIST special publication 1019, 6th edn. Tech. rep
32. Sikanen T (2019) PyroPython (version 0.01) [Computer software]. https://github.com/PyroId/PyroPython
33. Ghorbani Z, Webster R, Lázaro M, Trouvé A (2013) Limitations in the predictive capability of pyrolysis models based on a calibrated semi-empirical approach. Fire Saf J 61:274–288. https://doi.org/10.1016/j.firesaf.2013.09.007